ELSEVIER

Physica D 75 (1994) 55–73

PHYSICA D

Relevance of dynamic clustering to biological networks

Kunihiko Kaneko

Department of Pure and Applied Sciences, University of Tokyo, Komaba, Meguro-ku, Tokyo 153, Japan

Abstract

Network of nonlinear dynamical elements often show clustering of synchronization by chaotic instability. Relevance of the clustering to ecological, immune, neural, and cellular networks is discussed, with the emphasis on partially ordered states with chaotic itinerancy. First, clustering with bit structures in a hypercubic lattice is studied. Spontaneous formation and destruction of relevant bits are found, which give self-organizing, and chaotic genetic algorithms. When spontaneous changes of effective couplings are introduced, chaotic itinerancy of clusterings is widely seen through a feedback mechanism, which supports dynamic stability allowing for complexity and diversity, known as homeochaos. Second, synaptic dynamics of couplings is studied in relation with neural dynamics. The clustering structure is formed with a balance between external inputs and internal dynamics. Last, an extension allowing for the growth of the number of elements is given, in connection with cell differentiation. Effective time sharing system of resources is formed in partially ordered states.

1. Dynamical viewpoints

As is discussed in the preface, dynamical viewpoints have been appreciated in biological sciences. Here we need some logic to understand complex dynamical networks. Such studies are required from neural, immune, cellular, and ecological networks.

In neural systems, Tsuda has stressed the importance of (chaotic) dynamics in functions over several years [1–4]. Freeman has noticed the importance of the change of the degree of coherence of neural activities [5]. In the epilepsy, an ensemble of neurons exhibits a large spike due to the coherent oscillation of neural activities. Partial synchronization of nonlinear oscillations has been discovered in the visual cortex of a cat [6,7]. Vaadia and Aertsen [8,9] have found that the effective coupling among neurons varies temporally in a rather short time scale. They have found that the degree of synchronization among pairs of neurons change both temporally and by the choice of pairs.

In an ecological system, many species coexist in a network of food web. The population dynamics of species seems to be more stable as the complexity of network is larger, as Elton has discovered in the forest of England [10]. Furthermore the stability may not be sustained as a fixed point state [11], but is sustained in a dynamically changing state. In tropical rain forests, for example, there are a variety of species each of which has small population. Temporal variation of populations there is so large that the diversity in rain forests is often believed to be maintained only in a nonequilibrium state [12].

Similar interacting population dynamics is also important in the immune network, where Jerne proposed the network of antigens and antibodies [13]. Possibility of many attractors in such network system is discussed [14] in relation with spin glass type models [15], while

0167-2789/94/$07.00
SSDI 0167-2789(94)00066-Y

temporally successive switches of many states are discussed in [16].

At a somatic level, metabolic reactions often show nonlinear oscillations through catalytic reactions. In a developmental process and cell differentiation, interaction among cells is important besides the control by gene switches. Creation of diverse cells by the latter mechanism is often discussed in relation with many fixed point attractors [17], while dynamical viewpoints in cellular interactions are stressed in a recent experiment [18,19].

In these fields, studies on dynamic nonlinear networks are strongly requested, where a huge number of interacting nonlinear elements is involved. So far, spin-glass type models are used as a standard one for a system with many fixed-point attractors organized as a tree structure. With such models, static aspects or relaxation towards stationary states are studied. To address the dynamical problems listed above, however, we need studies of a system with many nonlinear interacting elements. The purpose of the present paper is to point out that the network of chaotic elements can provide a novel standard framework for a variety of biological networks with dynamical complexity.

The thesis of the present paper is motivated by the previous studies by the author on an ensemble of chaotic elements. There [20,21] it was found that clustering of synchronization is a general and important feature in globally coupled dynamical systems. Elements split into few or many clusters, in which their oscillations are synchronized. The number of clusters can differ by attractors, and by the strength of chaos. Complex partition into clusters is also found. This complexity is partly common with the spin glass type problems [22].

Generally speaking, there are three possibilities in clustering; phase, amplitude, and frequency of oscillations. For example, in the pure phase clustering, the amplitudes and periods of oscillations of elements are identical; only the phases of oscillations differ by clusters to which elements belong. So far the clustering we have studied does not purely consist of only one of the above three types. Phase, amplitude, and frequency clusterings are mixed, although the phase difference is most relevant to clusterings. In neural systems, it should be noted that synchronizations seem to split into clusters, as discussed as "gravitational clustering" by Vaadia and Aertsen [9]. These clusterings are rather complicated, although the phase differences seem to be important again.

In clustering it should be noted that identical chaotic elements differentiate spontaneously into different groups: even if a system consists of identical elements, they split into groups with different phases of oscillations. Hence a network of chaotic elements gives a theoretical basis for differentiation of identical elements, and provides a mechanism on the origin of diversity and complexity in biological networks.

The maintenance of diversity and complexity, besides their origin, is also an important problem in an evolutionary system. A dynamical mechanism of maintenance of diversity is recently proposed as homeochaos [25,26]. Here we also discuss a possible relationship between homeochaos and clustering.

Since two elements, once fallen in the same cluster, remain to be so, the relationship between two elements is fixed in nature. Besides the complexity in this fixed relationships dynamical changes of relationships and synchronizations are of importance in the biological problems listed above. Indeed, the network of chaotic elements shows dynamical complexity, when chaotic instability in each element is stronger; a typical example here is chaotic itinerancy [20,23,3,24] (see also Section 2).

The purpose of the present paper is to survey the relevance of the idea of clustering to biological systems. A rather personal view on biological networks along the above lines is given in Table 1. For the application of the idea, it is often necessary to extend the basic network of chaotic elements to different topology, to non-uniform

Field	View				
	One-to-one map	Static complex	Dynamic complex	Key concepts	Present paper
Neuroscience	Grandmother cell	Typical neural net	Dynamical correlation [4,1,8]	Clustering CI	Sections 5,6
Ecology	Niche-species	Random network [11]	Dynamic ecological network [25]	Clustering Homeochaos	Section 4
Immune	antigen-antibody	Jerne's net and [14]	Jerne's network and [16]	Homeochaos?	Sections 3,4
Development	gene-enzyme etc.	Kauffman's net [17]	GCM type [19]	Clustering Open Chaos	Section 7
Basic Model	–	Spin-glass type [15]	GCM type [20]	–	Sections 2,3

Table 1
Views of biological networks (personal perspective). CI=Chaotic Itinerancy.

elements, to synaptic couplings, and to systems with variable degrees of freedom.

In the next section we give a brief review of basic results of clustering, and chaotic itinerancy in globally coupled maps (GCM). In Section 3, the clustering idea is extended to a system with hypercubic topology. This extension is motivated by interacting population dynamics with mutation and its application to genetic algorithms. The formation of synchronized clusters strongly reflects the bit structure in the lattice. Indeed we will see self-organization and destruction of relevant bits and "don't care" bits by the chaotic itinerancy mechanism. In Section 4, we further extend the system in Section 3 to allow for a change of the coupling strength. The motivation for this extension comes from a system with interacting populations with mutation of mutation rates. By the last process, the coupling strength among elements (species) is effectively changed with time. It turns out that the system attains a dynamic stability allowing for diversity of many groups, by forming a feedback mechanism to adjust the coupling strength. This mechanism, called *homeochaos* turns out to be sustained by successive changes of clusterings. Sections 5 and 6 are devoted to extensions of our GCM to synaptic coupling cases, motivated by applications to neural systems. In Section 5, a globally coupled map with distributed coupling strengths is shown. Different types of clustering behaviors, from synchronized to completely desynchronized, are observed within a unique system. This observation opens up the possibility of controlling the degree of synchronization of elements according to inputs, by modifying the coupling strengths among the elements. Such control is carried out by a synaptic model introduced in Section 6, which is in a possible relationship with the synchronization by external inputs in the brain [8]. In Section 7, we study clusterings in a system with growing degrees of freedom, in connection with cell differentiation and growth. It is found that the dynamic clustering leads to growth of the number of cells by forming a time sharing system of foods (resources). Section 8 is devoted to a brief summary and discussions.

2. Brief review of globally coupled maps

The simpliest case of global interaction is studied as the "globally coupled map" (GCM) of chaotic elements [20,21]. An example is given by

$$x_{n+1}(i) = (1-\epsilon) f(x_n(i)) + \frac{\epsilon}{N}\sum_{j=1}^{N} f(x_n(j)), \qquad (1)$$

where n is a discrete time step and i is the index of an element ($i = 1, 2, \cdots, N$ = sys-

tem size), and $f(x) = 1 - ax^2$. The model is a mean-field-theory-type extension of coupled map lattices (CML) [27]. The above dynamics consists of parallel nonlinear transformation and a feedback from the "mean-field". It is equivalent to $y_{n+1}(i) = f[(1-\epsilon)y_n(i) + (\epsilon/N)\sum_{j=1}^{N} y_n(j)]$, with the aids of transformation $y_n(i) = f(x_n(i))$. In this form, one can see clear correspondence with neural nets: if one chooses a sigmoid function (e.g.,$\tanh(\beta x)$) as $f(x)$ and a random or coded coupling $\epsilon_{i,j}$, a typical neural net is obtained.

Through the interaction, some elements oscillate synchronously, while chaotic instability gives a tendency of destruction of the coherence. Attractors in GCM are classified by the number of synchronized clusters k and the number of elements for each cluster N_k. Here a cluster is defined as the set of elements in which $x(i) = x(j)$ [#1]. Each attractor is coded by the clustering condition $[k, (N_1, N_2, \cdots, N_k)]$. If we distinguish each element i, there are $N!/(N_1!N_2!\cdots N_k!)$ ways of the partitions for each clustering condition $(N_1, N_2, \cdots, N_k)$. We have exponentially many attractors for each clustering condition.

An interesting possibility in the clustering is that it provides a source for diversity. Even if the system is started from identical states, they split into different groups. In Section 7, we discuss the possibility of a role of clustering in cell differentiation.

In a globally coupled chaotic system in general, the following phases appear successively with the increase of nonlinearity in the system (a in the above logistic map case) [20]:

(i) *Coherent phase*: A coherent attractor ($k = 1$) has occupied (almost) all basin volumes.

(ii) *Ordered phase*: Attractors ($k = o(N)$ [#2]) with few clusters have occupied (almost) all basin volumes.

(iii) *Partially ordered phase*: Coexistence of attractors with many clusters ($k = O(N)$) and few clusters.

(iv) *Turbulent phase*: All attractors have N clusters.

In the turbulent phase, although $x(i)$ takes almost random values almost independently, there remains some coherence among elements. Indeed the distribution of the mean field $h_n \equiv (1/N)\sum_j f(x_n(j))$ does not obey the law of large numbers. The emergence of hidden coherence is a general property in a globally coupled chaotic system [21].

Existence of such coherence may be important to discuss about the EEG. In EEG, one measures a given average of neuronal (electric) activities. Since a firing pattern of each neuron is not regular (i.e., chaotic or random), the amplitude of the variation of EEG might decrease with the number of neurons involved in the average, as long as neuronal bursts are decorrelated. Since the number of involved neurons are so huge in the brain, the variation of average activity measured by EEG should be negligibly small, then. Still, we have observed a large enough amplitude of variation in EEG. This observation suggests that there remains some correlation among neuronal bursts. If each neuronal bursting were random, it would be hard to imagine a mechanism to keep such coherency. The above hidden coherence in globally coupled chaotic systems gives a possible origin of such coherence, where the amplitude of the variation of the mean field does not decrease with the number of elements.

In the partially ordered (PO) phase, complexity of partition into clusters is high. There are a variety of attractors with a different number of clusters, and a different way of partitions $[N_1, N_2, ..., N_k]$. We have measured the fluctuation of the partitions, using the probability Y that two elements fall on the same cluster. This Y value fluctuates by initial conditions. In the

[#1] Similar clusterings are also found in a system without local but with collective chaos [28].

[#2] $o(N)$ means that the quantity in concern is negligibly small compared with large N.

PO phase, this fluctuation is enhanced. Furthermore, the fluctuation remains finite even if the size goes to infinity [22]. It is noted that such remnance of fluctuation of partitions is also seen in spin glass models [15]. The increase of partition complexity at the partially ordered state may be important to study the relevance of the PO phase to biological systems.

We also note that the partition is usually inhomogeneous, and is organized as an inhomogeneous tree structure as in the spin glass model [20,15].

Besides the above *static* complexity, there emerges dynamic complexity in our model at the PO phase. The orbits make itinerance over ordered states via highly chaotic states. In the ordered states the motion is partially coherent. Our system exhibits *intermittent changes between the self-organization towards the coherent structure and its collapse to a high-dimensional disordered motion.* This dynamics, called *chaotic itinerancy*, has been found in a model of neural dynamics by Tsuda [3], optical turbulence [24], and in GCM. Here a number of ruins of low-dimensional attractors coexist in the phase space. The total dynamics consists of the residences at a ruin and a high-dimensional chaotic state interspersed between the two residences.

3. Bit clustering in hypercubic coupled maps (HCM): basis of chaotic genetic algorithm

Let us discuss some (population) dynamics of many individuals, coded by genes. If genes are represented by a bit sequence, the mutation process in gene space is given by the diffusion in the bit sequence. When some nonlinear population dynamics is included to take into account of the saturation, competition, or prey-predator (host-parasite) interaction, the total population dynamics is given by the local nonlinear dynamics and the diffusion process on the hypercubic lattice of length 2, corresponding to the bit sequences. The minimal model for this process is given by the following coupled map on a hypercubic lattice:

$$x_{n+1}(i) = (1-\epsilon) f(x_n(i)) + \frac{\epsilon}{K} \sum_{j=1}^{K} f(x_n(\sigma_j(i))), \tag{2}$$

where $\sigma_j(i)$ is a "species" whose jth bit is different from the species i (with only one bit difference), and K is the total bit length of species (the number of total "species" is 2^K). We use a decimal representation of bit sequence often; for example 42 stands for the sequence 101010, and $\sigma_2(42) = 40$.

The present model may be relevant to genetic algorithms [31], where the population of bit-strings changes according to their fitness. The model is also of theoretical interest, since it lies between globally coupled and locally coupled models (CML) [27]: In a global coupled chaotic system, we have N connections per element, while a d-dimensional CML (with nearest neighbor coupling) has $2d = o(N)$ connections per element. In our hypercubic system with $N = 2^K$ elements, we have $K = \log_2 N$ connections per elements [30].

In the model (2) we have often observed a state with few synchronized clusters when the nonlinearity parameter a is not large. (The phase diagram with respect to the parameter space (a, ϵ) will be given later). Here a synchronized cluster means, as in Section 2, that two elements in the cluster oscillate in complete synchronization, i.e., $x_n(i) = x_n(j)$ for two elements i and j in the cluster. In the present case, the split to two clusters is organized according to the hypercubic structure. For example, the following types of clusterings are observed.

(A) 2 clusters by 1 bit.

Elements split into two synchronized clusters. All elements in each cluster oscillate in synchronization as shown in Figs. 1a and 1b, where successive snapshots of $x_n(i)$ are plotted as a function of i.

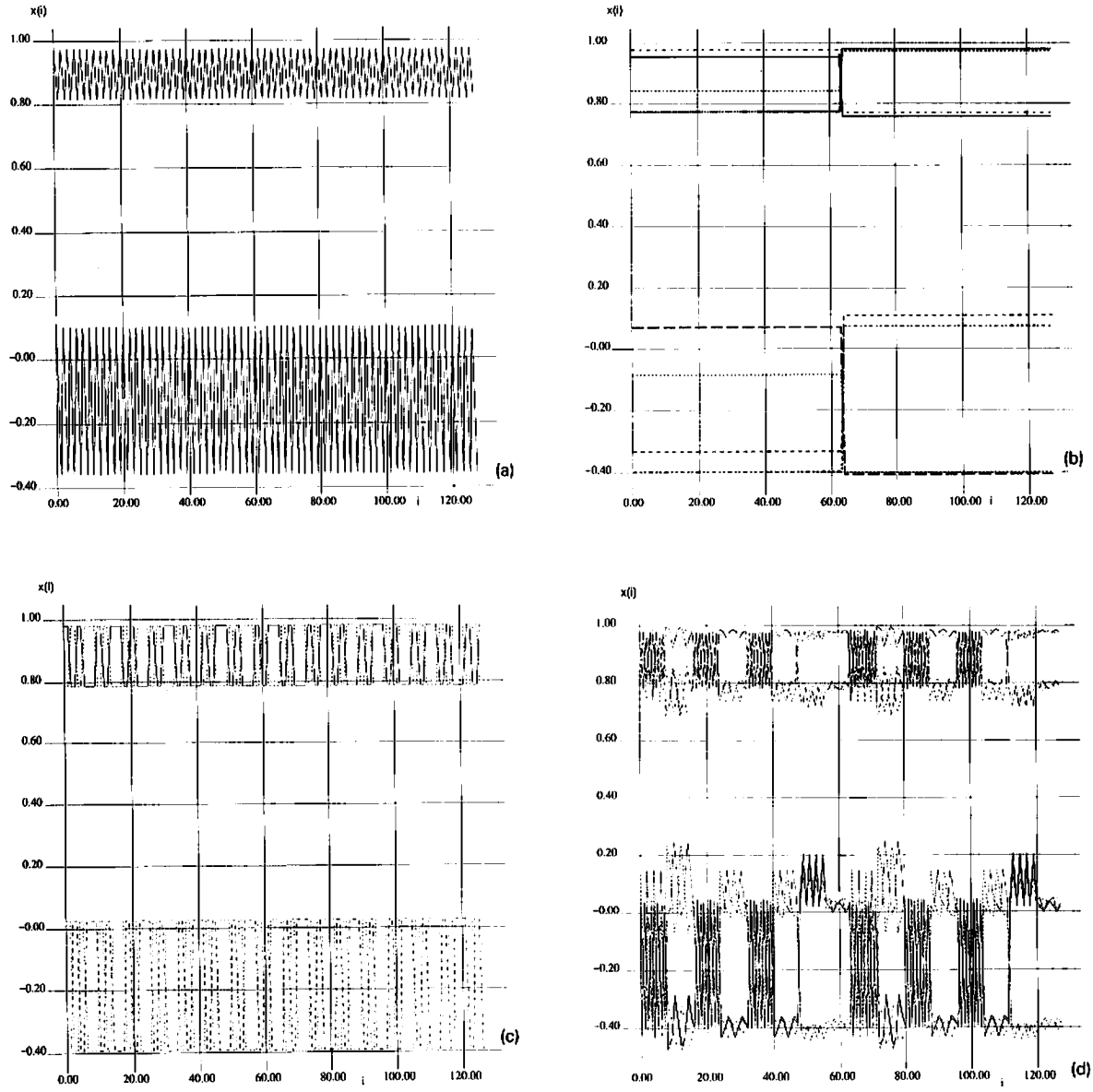

Fig. 1. Snapshot $x(i)$ of hypercubic coupled map (2) with $k = 7$ and $a = 1.5$, plotted as a function of i, decimal representation of the bit string. $\epsilon = .4$ for (a) and (b), $\epsilon = .3$ for (c) and (d). (a) Two successive time steps (after 100000 steps) are overlaid for a two-cluster attractor, split by the condition $******0$ and $******1$. (b) 8 successive time steps are overlaid for a two-cluster attractor, split by the condition $0******$ and $1******$. (c) 8 successive time steps (after 100000 steps) are overlaid for a two-cluster attractor, split by the XOR condition [$***0*0*$ or $***1*1*$] and [$***0*1*$ or $***1*0*$]. (The attractor is a stable cycle with period-4). (d) 8 successive time steps are overlaid for a 12-cluster attractor. (The attractor is chaotic).

Such clustering into two is frequently observed in a globally coupled map system, where arbitrary partition of elements into two clusters is possible. In our HCM, the partition is governed by the spatial structure in the hypercubic lattice. For example, elements may be grouped into two clusters with $**0***$ and $**1***$, ($*$ means that the symbol there is either one or zero), each of which has 2^{K-1} species. If the elements split into the group of $******1$ and $******0$ for example, the snapshot of $x(i)$ shows a zigzag structure (with period 2) if plotted as a function of the decimal representation i (see Fig. 1a), while the split by the Kth bit leads to a periodic structure with period 2^K (see Fig. 1b). This clustering is formed by cutting the K-dimensional hypercube by a hyperplane.

(B) 2 bit clustering.

Depending on initial conditions and parameters, the number of relevant bits for clustering can be larger than the case (A), as well as the number of clusters. In the 2 bit clustering there are following possibilities:

(B0) 4-cluster state with two relevant bits. This case is just a direct product of the previous case (A). The hypercubic space splits by two hyperplanes. Elements split into four clusters, for example, coded by $01*****$, $10*****$, $11*****$, and $00*****$.

(B1) 2-cluster with 2 bits (XOR construction).

We have also found an attractor with 2 clusters with the use of 2 relevant bits. For example the elements split into the groups (i) $10*****$ or $01*****$ and (ii) $00*****$ or $11*****$. This split corresponds to the construction of XOR (exclusive or) with the use of 2 relevant bits (see Fig. 1c).

(B2) 3-cluster with 2 bits.

We have also found a 3-cluster state with 2 bits, constructed for example as (i) $10*****$ or $01*****$ (ii) $11*****$ and (iii) $00*****$.

It should be noted that not all partitions are possible in the HCM. Even if we start from an initial condition with a given clustering condition, the synchronization condition ($x(i) = x(j)$ for i, j belonging to a same cluster) is not satisfied at the next step, for most of such initial conditions. In contrast with the GCM case, not all possible partitions can be a (stable or unstable) solution of the evolution equation.

One can easily check that the synchronization is preserved for the clustering (A), (B0), (B1), and (B2). Generally the clustering should be constructed as a combination of hyperplane cuts, and the condition of a cluster is written as a bit representation with the symbol "$*$", corresponding to the "don't care" bit "#", in genetic algorithms [31].

(C) 3 bit and higher (K) bit coding.

Clustering with the use of bits more than 2 are constructed in a similar manner. Most clusterings observed here are direct products of (A) or (B1)–(B3).

(C1) parity check: 2 clusters from K bits.

Elements split into two groups according to the parity of the number of 1's in each bit representation. For example, elements split into two clusters as follows: (i) 000, 011, 101, 110 and (ii) 001 010, 100, 111, for $K = 3$. The clustering, thus gives a parity check. It is a hypercubic version of the zigzag (1-dim) or checkerboard (2-dim) pattern [27].

(C2) Hamming distance code: $K + 1$ clusters from K bits.

Elements split into $K + 1$ clusters according to the Hamming distance from an element. This is a straightforward extension of the clustering (B3). For example, elements split into 4 clusters as follows (i) 000 (1 element) , (ii) 001, 010, 100 (3 elements) , (iii) 011,101, 110, (3 elements) and (iv) 111 (1 element) , for $K = 3$. This clustering is constructed by the cuts by K parallel hyperplanes.

An attractor with many clusters is often constructed by a direct product of combinations of (A0), (C1), and (C2) , that is of (0) 1 bit code by a hyperplane cut, (1) Parity check and (2) Hamming distance cuts (see for example Fig. 1d) for a 6-cluster attractor).

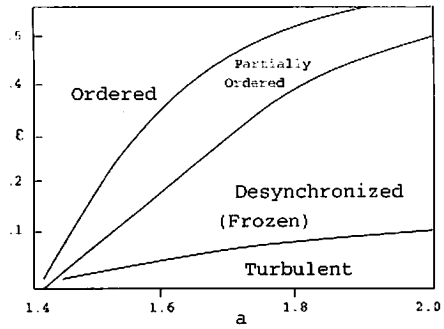

Fig. 2. Rough phase diagram of the hypercubic coupled map (2) with $K = 7$. Obtained by measuring the number of clusters for attractors starting from 10 different sets of initial conditions. The calculation is carried out by incrementing the parameters a and ϵ by 0.02.

A very rough phase diagram of our hypercubic coupled map is given in Fig. 2. Transitions are found successively through ordered, partially ordered, and desynchronized phases, as in the GCM in Section 2. In the figure, both the turbulent and frozen desynchronized phases have attractors with $k = N$, i.e., with full desynchronization. In the frozen desynchronized phase, oscillations are chaotic but they keep a period-2 band motion. The phase relationship of oscillations (of period-2 band) is preserved in the same way as the frozen random phase of CML [27]. In one domain $x_n(i)$ changes in time as large–small–large$\cdots$, while it changes in a reverse phase in the other domain. As in the frozen phase of CML [27], these domains of the same phase relationship do not change in time (see for details [29]). In this respect, our hypercubic coupled map has both the natures of locally and globally coupled maps.

In the partially ordered phase, there are a variety of clusterings with a large number of clusters. There some elements stay very close and oscillate almost synchronously over some time steps, but then they are separated due to chaotic instability. In a very narrow regime around $a \approx 1.53$ and $\epsilon \approx .3$, we have found a chaotic itinerancy state, where relevant bits change according to temporal evolution. In Fig. 3, change of relevant bits for the clustering is seen. In Fig. 3a,

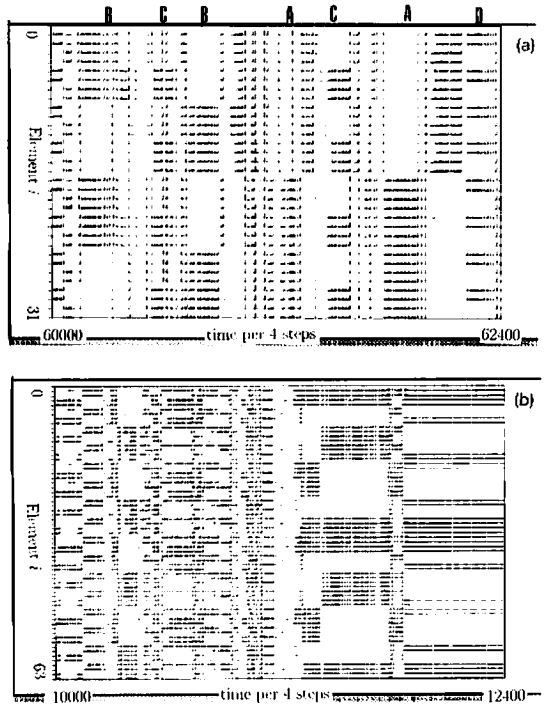

Fig. 3. Space-time diagram for the coupled map lattice on a hypercubic lattice (2) with $\epsilon = .3$. On the corresponding pixel at a given time and element, a bar with a length proportional to $(x_n(i,j) - 0.1)$ is painted if $x_n(i,j) > .1$. Every 4th time step is plotted. (a) $a = 1.525$, $K = 5$ (i.e., $N = 2^5$). Plotted from time steps 60000 to 62400. The itinerancy does not stop (we have checked up to 500000 steps). (b) $a = 1.54$, $K = 6$ (i.e., $N = 2^6$). Plotted from time steps 10000 to 12400. The system is attracted to a two-cluster state around the time steps 12100, and remains the state forever.

for example, the system approaches a two cluster state given by $*0****$ and $*1****$ denoted as the stage B. Then the state switches as $B \to C \to B \to A \to C \to A \to D \to \cdots$, where the stage A means the split into two clusters $0*****$ and $1****$, the stage C into $**0**$ and $**1**$, and D into $0****$ and $1***$.

When the number of bits K is larger than 5, this state is seen only as very long transients before the system finally falls on an attractor with few clusters. For example, see Fig. 3b, where the system finally is attracted into an exact two-cluster state around 12100 steps and remains there forever.

With the introduction of external inputs to

each element, it is also possible to have a clustered state following the external information [29]. Let us assume, for example, that the external inputs are constructed by common inputs for some bits ("relevant bits") and "noise" parts for all bits (see e.g., Eq. (9) of Section 6). By applying this class of inputs, our system is attracted to a state clustered by the relevant bits. Relevant information is thus extracted through this process spontaneously, which is stored as the relevant bits in the clustering.

4. Homeochaos and clustering: dynamic maintenance of diversity

In a system with interacting population dynamics, it is an interesting question how diversity of genes are maintained. In [25], we have proposed a concept "homeochaos" as a mechanism for sustaining dynamic stability with diversity. Population dynamics models with interaction among species, mutation, and mutation of mutation rates have been studied [25,26].

In particular, we take a 2-dimensional map for local dynamics here, since we are interested in the interaction between hosts and parasites (or preys and predators). Each individual has a gene coded by a bit sequence as in Section 3. We assume that the parasite can attack a host only if their bit strings are completely matched. By this restriction, we can have a 2-dimensional map for the local population dynamics of each bit string. To be specific we have studied the model

$$h'(i) = a[1 - h(i)][h(i)]\exp(-\beta p(i)), \quad (3)$$

$$p'(i) = h(i)[1 - \exp(-\beta p(i))], \quad (4)$$

instead of the 1-dimensional logistic map in Section 3. Here the set of variable $(h(i), p(i))$ gives the population of the host and parasite of the "species"[#3] i. The term $\exp(-\beta p(i))$ represents the fraction that is killed by the corresponding parasite i.

Further we assume that each "species" i can have different mutation rates, in other words, each is coded by (i, j) rather than i, where j denotes the mutation level. Thus our system is described by a set of populations of "species" i and the mutation level j denoted by $\{h_n(i, j), p_n(i, j)\}$ at time n.

Since the mutation level does not affect the interaction, the local dynamics is obtained straightforwardly from (3) and (4); First we introduce $h_n^s(i) = \sum_j h_n(i, j)$ and $p^s(i) = \sum_j p_n(i, j))$, the sum of the populations of each "species" over all mutation levels. Then the local dynamics of $h_n^s(i)$ and $p_n^s(i)$ obey exactly (3) and (4). The local dynamics $h(i, j) \to h'(i, j)$ is given by multiplying the dynamics of $h^s(i)$ by $h_n(i, j)/h_n^s(i)$, the fraction of the population of the level j. (Of course the dynamics $p(i, j) \to p'(i, j)$ is given by multiplying the corresponding equation by $p_n(i, j)/p_n^s(i)$.)

After this population dynamics each group (i, j) has a mutation change from its nearest neighbor point in the hypercubic lattice $\sigma_k(i)$ in the same way as in Section 3, with the rate given by the mutation level j (here we assume $\epsilon_j = 2^{(j_{\max}-j)/4}$ and $j_{\max} = 30$). Furthermore we assume that the mutation level also changes by mutation, given by a diffusive coupling between neighboring levels of j ($j \to j \pm 1$), with the (mutation) rate ϵ_j (see [26]).

Thus the total dynamics (which is a little bit complicated but is straightforwardly obtained) is given by the coupled map lattice with the diffusive coupling by the mutation. The coupling strength ϵ_j depends on the level j, as stated, and there is also diffusive coupling between neighboring mutation levels $j \pm 1$.

Through the mutation of mutation rate, the mutation level is sustained at a high level, with some temporal fluctuation. As is studied in [26], weak high-dimensional chaos is observed here, which affords the stability with diversity. All "species" i keep their finite population with

[#3] Here we use the term "species" as types of bit string, not in the strict sense in biology.

temporal variation. This stability with diversity is called "homeochaos", and is proposed to be essential to the stability of biological networks [25,32]. Examples may cover not only ecological systems but also immune networks, where high mutation rates are physiologically confirmed.

In Fig. 4, we have plotted snapshots of $h^s(i)$ successively. At time step 9000 (Fig. 4a), populations split into 7 clusters with the bit condition $\circ * \circ * * * \circ$. ($\circ$ shows a relevant bit to clustering.) The first, third, and last bits are relevant to clustering. (Among possible $2 \times 2 \times 2$ clusters, two groups $0 * 1 * * * 1$ and $1 * 1 * * * 1$ are fused to form a single cluster. Thus the number of clusters is seven.) At time step 18000 there are 12 clusters with 4 relevant bits as $\circ \circ * * * * \circ \circ$, while 4 clusters exist at 21000 with the condition $\circ * * * * * \circ *$ [#4]. We also note that a highly chaotic state is interspersed between two clustered states. An example of the snapshot pattern there is given in Fig. 4d. Summing up, we have observed changes of bit clustering with chaotic itinerancy .

In Fig. 5a, we have also plotted the time series of the effective degrees of freedom, defined as the number of clusters with a given (finite) precision; i.e., when $h^s(i)$ and $h^s(j)$ agree within the precision, they are assumed to be the same "effective" cluster. Drops of the effective degrees give the emergence of "almost" clustered states as in Fig. 4a. Corresponding time series of the average mutation level is given in Fig. 5b.

This type of chaotic itinerancy is seen in a narrow parameter regime in the previous section (e.g. only around $a \approx 1.52$ in the model in Section 3 for $\epsilon \approx .3$, as long transients. In the above two variable model, it is seen only around $a \approx 3.75$ (as long transients) when the mutation rate is fixed (e.g., at $j = 25$). On the other hand, such behavior is seen over all regimes for $a > 3.5$, with the inclusion of mutation of mutation rates. Hence there must be a mechanism to adjust the effective coupling strength (i.e., the mutation rate here) so that the system stays around at the partially ordered state. Such adjustment mechanism is essential to homeochaos.

A high mutation level (i.e., large coupling ϵ_j) is necessary to have a state with few clusters. As the mutation level is increased, the oscillations tend to be synchronized (recall that the number of clusters in coupled maps decreases with the increase of coupling strength; see Sections 2 and 3). By examining the change of mutation rates (coupling strengths) and the change of clustering in detail, it is possible to propose the following feedback mechanism which keeps the system at the partially ordered state:

(i) increase of mutation level leads to the synchronization of population oscillation, since the coupling is increased;

(ii) the synchronization leads to decrease of the mutation level;

(iii) the decrease of mutation level leads to the split of synchronized clusters, since the coupling is decreased (see Sections 2 and 3);

(iv) split of clusters is associated with the irregular temporal dynamics, which leads to increase of mutation level, and then to (i) [26].

This feedback mechanism is necessary to maintain our system at the partially ordered state with the chaotic itinerancy of bit clusterings. Since such partially synchronized state is thought to be important in biological networks [3,9], the above mechanism for evolving to, and maintaining, the state is important. It is an interesting future problem to elucidate a similar feedback mechanism in other biological networks.

5. Extensions to coupling forms with more complicated structure

In a biological system, the elements are not homogeneous. It is often necessary, then, to assume that local dynamics or a coupling strength depends on elements. Also time dependence of

[#4] Small difference by the last bit is also detectable, though. Including this difference here are 8 clusters.

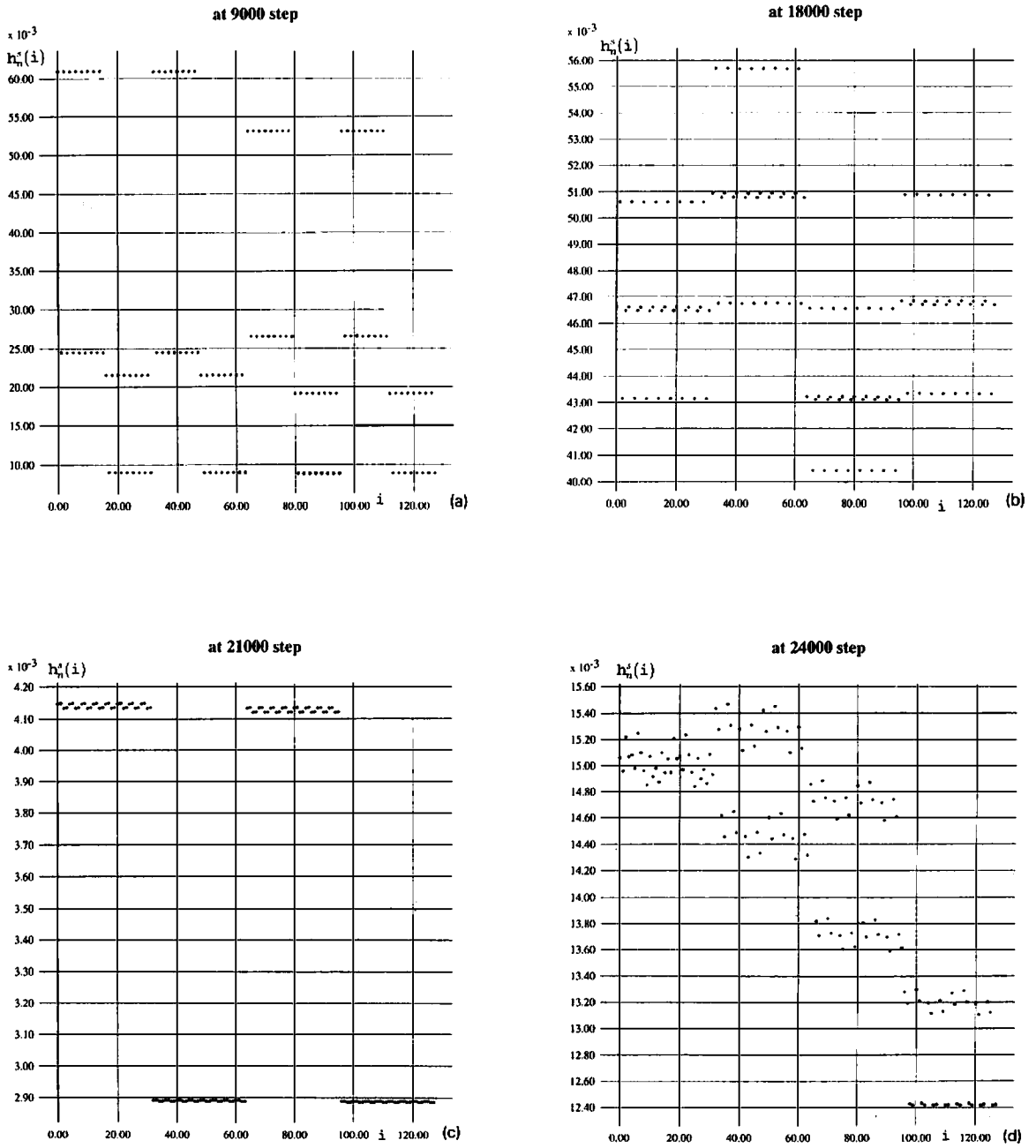

Fig. 4. Snapshot plots of $h_n^s(i)$ for the model with mutation of mutation rates described in the text. $a = 3.5$, $\beta = 7.0$, $k = 7$ and $j_{max} = 30$. (a) time step 9000, (b) 18000, (c) 21000, (d) 24000.

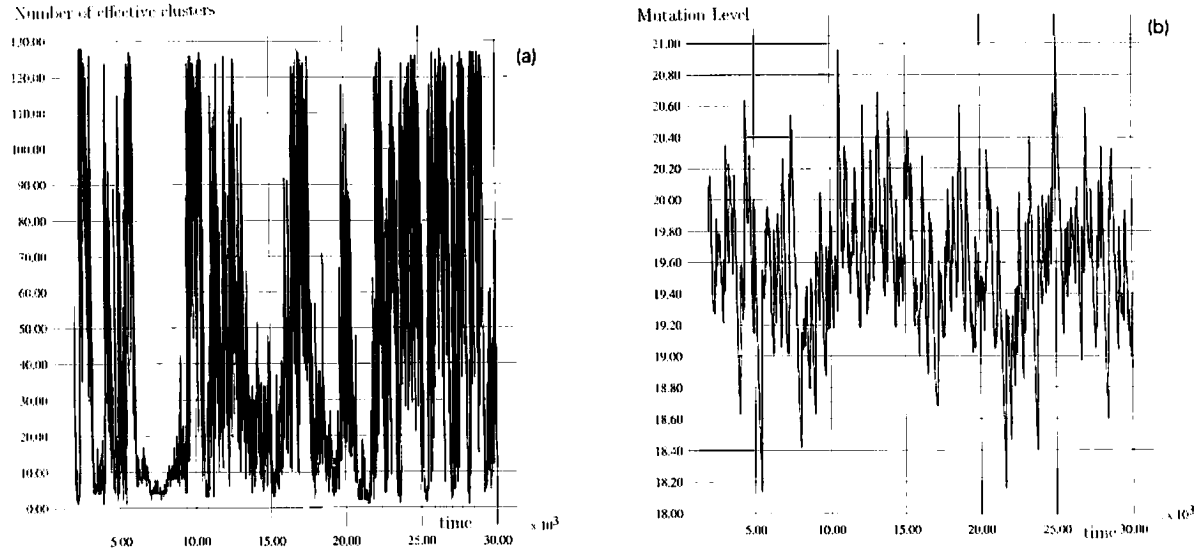

Fig. 5. (a) Time series of the effective degrees of freedom, corresponding to the simulation of Fig. 4. An effective cluster is defined as follows; if $x(i)$ and $x(j)$ agree within the precision 2^{-13}, successive drops of the degrees are seen, which corresponding to a bit-clustered state like Fig. 4a). (b) Corresponding temporal evolution of the average mutation level j.

such parameters may be necessary.

Here we extend the previous GCM by allowing for inhomogeneous parameters by elements, instead of identical parameters for all. There are two possibilities here; choice of distributed $a(i)$ instead of a constant nonlinearity a or distributed $\epsilon(i)$ instead of a constant coupling ϵ. For the latter case, the model is given by

$$x_{n+1}(i) = [1-\epsilon(i)]f(x_n(i)) + \frac{\epsilon(i)}{N}\sum_{j=1}^{N} f(x_n(j)). \quad (5)$$

In Fig. 6 we have plotted a snapshot of $x_n(i)$ for a system with homogeneously distributed coupling over $[\epsilon_{\min}, \epsilon_{\max}]$ (i.e., $\epsilon(i) = \epsilon_{\min} + (\epsilon_{\max} - \epsilon_{\min})(i/N)$). As is seen, the clustering structure depends on the coupling strength at each element. Elements with large coupling ($\epsilon > .22$) form a single synchronized cluster, while the number of clusters increases successively with the decrease of the coupling strength at the element. Such clustering bifurcation looks similar with the phase change (i) → (iv) in Section 2. However, this is not a trivial extension. The clustering change in Section 2 is the bifurcation with system parameters, while the change here is included in a single network system, where all the elements therein are connected by a unique mean field. Still "internal" bifurcation among elements occurs here. At the edge parameter region between clustered and turbulent states ($\epsilon \approx 0.12$ in Fig. 6), the motion is rather complicated with chaotic itinerancy. Desynchronized bursts emitted from the elements with smaller $\epsilon(i)$ flow to elements with larger $\epsilon(i)$, where clustering can change in time.

The behavior discussed here is also seen in a model with the distributed nonlinearity, i.e., $a(i) = a_{\min} + (a_{\max} - a_{\min})(i/N)$. The "internal" bifurcation from the ordered state to the turbulent one occurs with the increase of the index of elements i.

If the range of distribution of coupling is small, the behavior there approaches that in the previous section. According to the width of the coupling range variety of clusterings decreases. We note that the hidden coherence still emerges in

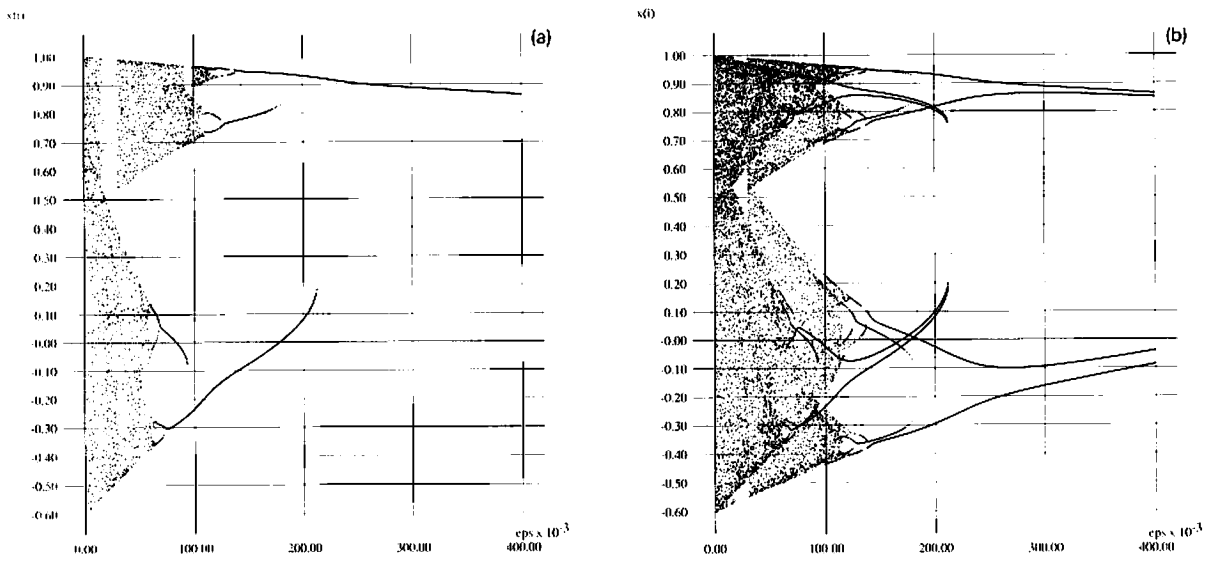

Fig. 6. Snapshot of the globally coupled map (5), with $a = 1.6$, $N = 10^5$. $x_n(i)$ at the time step $n = 5000$ is plotted as a function of i. The coupling $\epsilon(i)$ is ordered as $\epsilon(i) = 0.4(i/N)$. (b) Successive snapshots $x_n(i)$ at the time steps 5001, 5002, 5003, and 5004 are overlaid.

the turbulent state, even if the parameters a or ϵ are distributed [21].

6. Synaptic dynamics

In traditional neural networks, coding is assigned at firing patterns $x(i)$, while the synaptic change and memory are assumed to be assigned on the interaction strength between two elements i and j. Recently there are some arguments that dynamical coding, given by the correlation between $x(i)$ and $x(j)$, may be important [8,9]. Then it may be interesting to pursue this "converse" limit: in other words, let us assume that the synaptic change and memory are assigned on the coupling $\epsilon(i)$ at i, not on the interaction between i and j. Thus we take the following model:

$$x_{n+1}(i) = [1 - \epsilon_n(i)]f(x_n(i)) + \frac{\epsilon_n(i)}{N}\sum_j f(x_n(j)), \tag{6}$$

where $\epsilon_n(i)$ is in-(de-)creased according to inputs on the ith element. To be specific, we take the following dynamics; first increase the coupling to the mean field, according to the input $s_n(i)(>0)$ by

$$\epsilon'(i) = \epsilon_n(i) + \gamma s_n(i), \quad \text{with } \gamma > 0, \tag{7}$$

and then rescale the coupling so that the average of $\epsilon(i)$ is conserved:

$$\epsilon_{n+1}(i) = \epsilon_0 \times \frac{\epsilon'(i)}{\sum_j \epsilon'(j)}. \tag{8}$$

Indeed the latter equation is introduced only for a suppression, and may be replaced by other forms to suppress the overgrowth of $\epsilon_n(i)$. What we need here is a mechanism for (a) the suppression of an indefinite increase of coupling $\epsilon(i)$ and (b) the competition among elements for the increase of coupling.

When common inputs are applied to elements $i_0 \le i \le i_1$, synchronization degree of the oscillations $x_n(i)$ for $i_0 \le i \le i_1$ increases. Depending on the input strength, two elements i, j with common inputs often synchronize completely. After inputs are eliminated, a pair of (almost) synchronized elements remains coherent or cor-

related. We have thus achieved clustering according to inputs [33]. This clustering is often preserved even if the coupling $\epsilon_n(i)$ is again restored to be homogeneous.

Generally, the clustering is formed according to the structure of inputs. We have made some simulations with correlated inputs in p groups per N/p elements. In particular we take

$$s_n(i) = R_n(\mathrm{int}(i/p)) + r_n(i), \tag{9}$$

where $R_n(\ell)$ is a random signal (depending on the argument ℓ), with the amplitude 1. With the form $R_n(\mathrm{int}(i/p))$, common inputs are applied to each group $kN/p < i \leq (k+1)N/p$, while r_n is a noise depending on elements but with much smaller amplitude δ ($\delta < 1$). Adopting this form, inputs are random, but are strongly correlated within each group of N/p elements. In Fig. 7 we have plotted the spacetime diagram when these inputs are applied ($p = 4$). Correlated motion within each N/p elements is seen. Some of the correlation remain even after the inputs are eliminated (see Fig. 7b).

To see the correlation in oscillations $\{x_n(i)\}$ more quantitatively, we introduce the difference matrix

$$\Delta_{ij} = \langle (x_n(j) - x_n(i))^2 \rangle, \tag{10}$$

where $\langle \cdots \rangle$ is temporal average. The difference matrix is plotted in Fig. 8 for the inputs in the above structure. We note that the partial clustering is formed according to the structure of inputs, as long as the number of input groups is small (i.e., typically $p \leq 8$). This organization is not trivial since we have not imposed any direct change of the coupling to increase the coherence among elements with correlated inputs. No enhancement of the connection between pairs is required here. Indeed, given an element, the coupling strength takes a same value for any pair between it and other elements.

The formation of clustering according to inputs works well if the parameters a and ϵ_0 are chosen so that the number of clusters there is not far from the expected cluster number by inputs.

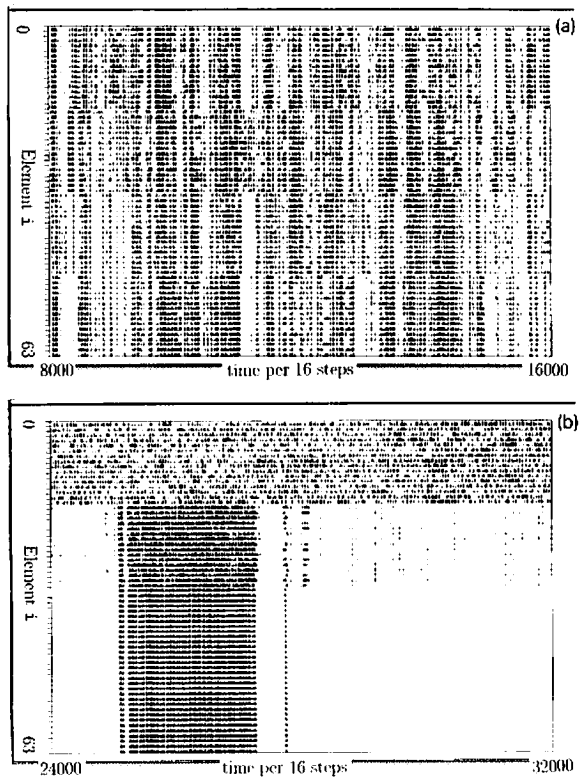

Fig. 7. Space-time diagram for the globally coupled map Eq. (6) with Eqs. (7) and (8) with the inputs Eq. (9), with $p = 4$. $a = 1.85$, $\delta = 0.1$, $\gamma = 0.1$, $N = 128$. On the corresponding pixel at a given time and element, a bar with a length proportional to $(x_n(i,j) - 0.1)$ is painted if $x_n(i,j) > .1$. (a) Every 16th time step is plotted from 8000 to 16000. (b) Continued from a), after the inputs are stopped at the time step 20000. Over the time steps 24000 to 32000.

If the number of clusters at the corresponding a and ϵ_0 values is smaller than that of the inputs, some of the groups are fused into a same cluster. Relationships between some input groups are self-organized by the internal dynamics. Generally, the above clustering is formed by the balance between internal dynamics and the external inputs. In Fig. 8a, for example, 3 out of 4 input groups are mapped into the clustering, but the other group is not clearly mapped. In Fig. 8b, two of the four input groups are mapped, while the other two split into smaller clusters.

There is a recent report of an interesting experiment by Hayashi [34], where synchronization

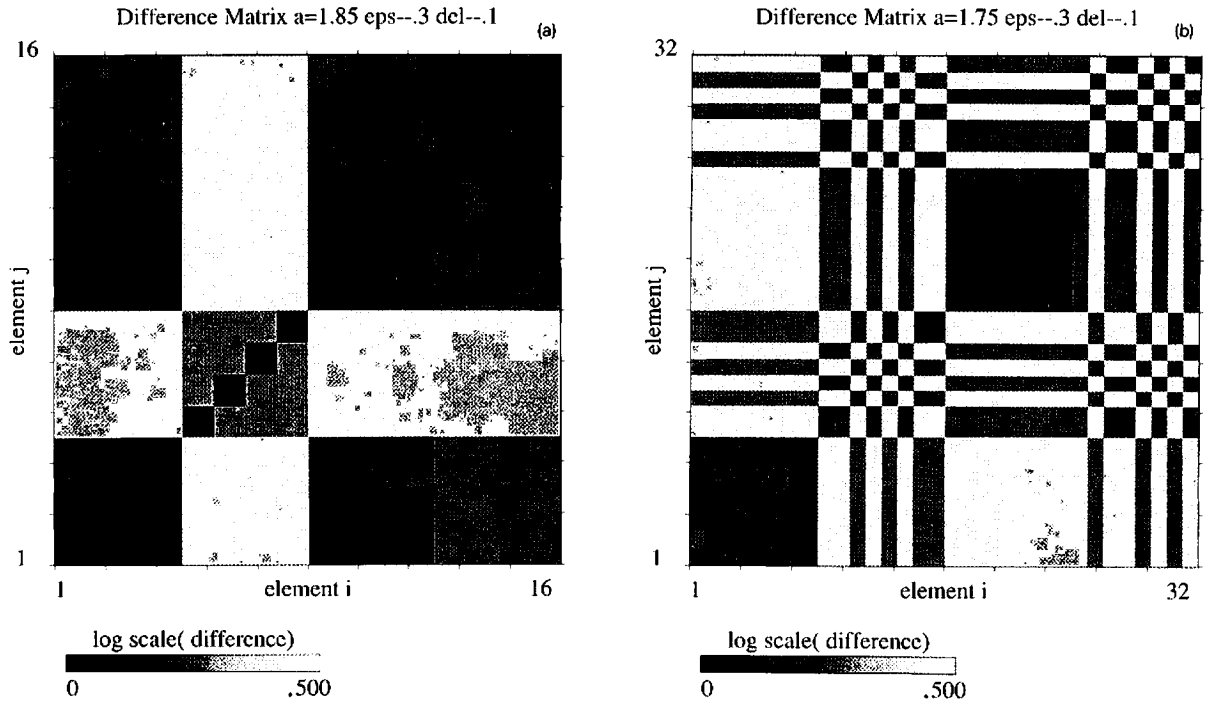

Fig. 8. Difference matrix Eq. (10) averaged over 20000 steps, after inputs of Eq. (9) with $p = 4$ and $\delta = 0.1$ are applied for 20000 steps. The synaptic dynamics (7) and (8) are used with $\epsilon_0 = 0.3$, and $\gamma = 0.1$ (a) $N = 16$, and $a = 1.85$ (b) $N = 32$, and $a = 1.75$.

among neurons is increased when a rat is continuing a task with a feedback to the brain. In our model this corresponds to the growth of $\epsilon(i)$ for all elements. With further continuing the task, the synchronization reaches its maximum, and the rat's brain goes to an epileptic state, where the information processing ability is lost. In our model complete synchronization would be attained if the suppression term (Eq. (8)) were not included. To avoid such catastrophe, we have to introduce some mechanisms to suppress the increase of ϵ in our model. We may expect that such mechanism exists in the real brain, and that its breakdown leads to the epilepsy.

7. Growing coupled maps: origin of diversity and differentiation

One missing feature in our network of chaotic elements so far, is the possibility to change the degrees of freedom themselves. In biological systems, often the number of elements itself varies. Such growth of elements is also seen in the economics, where the number of agents can change in time through reproduction and extinction. Here we study a very simple model with the growth of the number of elements, taking a coupled map model. A related but more realistic model for cell division and differentiation is given in [19].

We assume that there is a variable $x(i)$ determining the cell state, and that cells compete with each other for a source term s. Source term s is supplied from outer environments with a constant rate c. The ability to get this source depends on the internal state $x(i)$, with some nonlinear function $f(x)$. Thus the dynamics of each $x(i)$ is given by

$$x_{n+1}(i) = x_n(i) + f(x_n(i)) + S_n, \qquad (11)$$

$$S_n = \frac{c - \sum_j f(x_n(j))}{N}. \qquad (12)$$

The term $x_{n+1}(i) - x_n(i) = f(x_n(i)) + S_n$ gives a source term that the element i takes at the time step n. The second condition assures $\sum_i \{x_{n+1}(i) - x_n(i)\} = c$, that is, the sum of the source term balances with that supplied externally.

Further we introduce the following dynamics for cell division and death.

(A) Divide the cell i if $x_n(i) > T_g$. After the division, x of the cell i and the new element $N + 1$ is assigned to be $(x_n(i) - T_g)/2 + \delta$ and $(x_n(i) - T_g)/2 - \delta$, with a very small random number δ.

(B) Remove the cell i if $x_n(i) < T_d$. Here we fix $T_g = 1$ and $T_d = 0$, although our results are essentially independent of the choice of T_g and T_d. The function $f(x)$ is chosen to be $f(x) = \frac{K}{2\pi} sin(2\pi x)$

Time series of the number of cells and the effective number of clusters are plotted in Fig. 9, while the maximal and average numbers of cells are plotted as a function of K in Fig. 10. We note that the growth is maximal around $K \approx 4.3$.

In the corresponding coupled map model with a fixed number of elements (i.e., globally coupled circle map [23]), the system is in a coherent phase for $K < 2$, at the ordered phase for $2 < K < 4.1$, at the partially ordered phase around $4.1 < K < 4.4$, and at the turbulent phase for $K > 4.4$.

Thus our result suggests that the growth is enhanced at the partially ordered state. If oscillations of all elements are synchronized, they compete for the source term at the same timing. This hard competition is not good for an effective use of resources. By the clustering, a sort of time sharing system is constructed. Thus resources are effectively used with some ordering by elements. On the other hand, if the elements are completely desynchronized, no ordering for the use of resources is possible. In this case effective use of resources is again impossible. Thus the growth

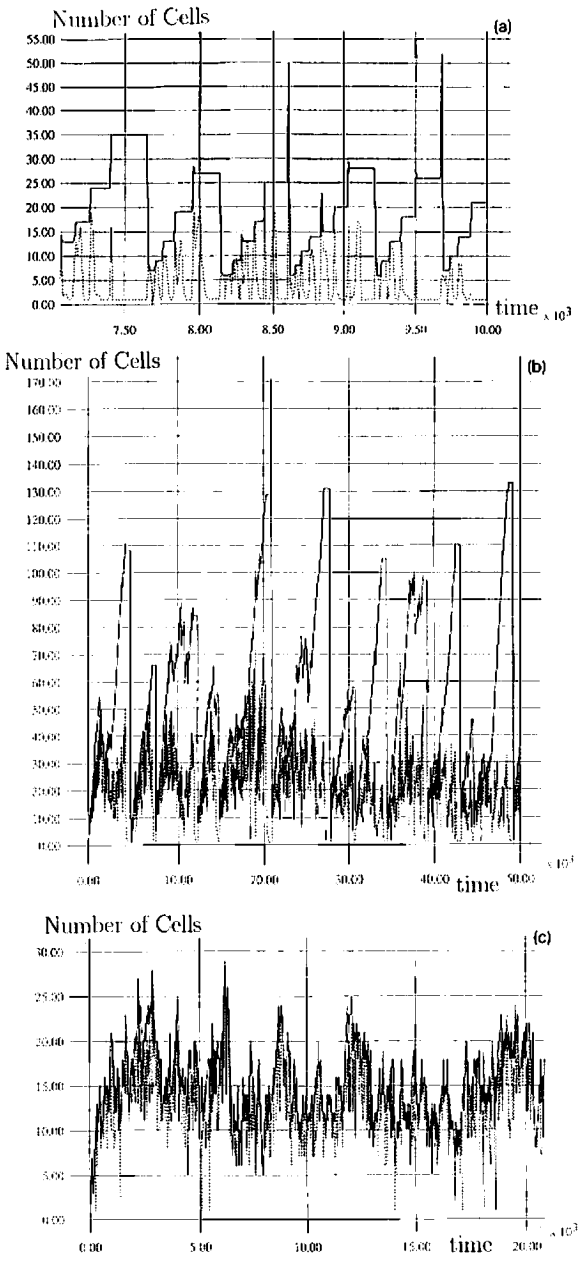

Fig. 9. Temporal evolution of the number of cells N (thick line) and the effective cluster number (dotted line). The effective cluster number is defined as that of clusters with the precision 10^{-4} (checking the equality between $x(i)$ and $x(j)$ with this precision). Simulations are carried out with the use of Eq. (11) with $c = 0.1$, starting from one cell ($N = 1$). (a) $K = 2.4$, (b) $K = 3.35$, (c) $K = 3.45$

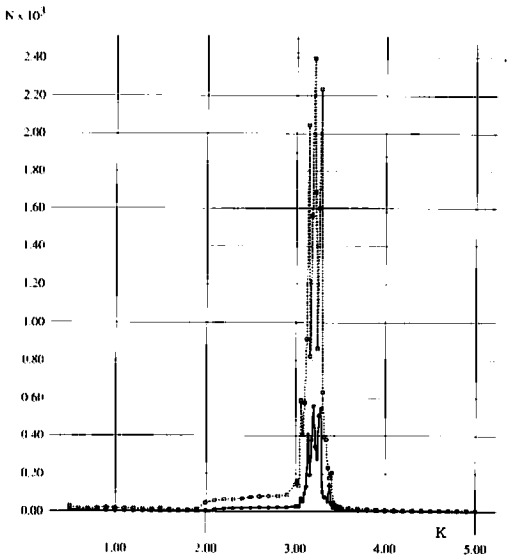

Fig. 10. The average (thick line) and maximal number of cells over the time steps 5000 to 15000. Simulations are carried out with $c = 0.1$, and starting from one cell.

is enhanced at the partially ordered state, where synchronization is lost but there remains some ordering.

At the partially ordered state, typical clustering is quite inhomogeneous. Some elements form a large cluster, while there are many other elements with desynchronization. Cells belonging to a large synchronized cluster grow slower than desynchronized cells. When these synchronized cells divide, the number of cells suddenly increases by N_1, the number of elements in the cluster. This increase causes a hard competition for resources, and often leads to spontaneous death of many cells. Such multiple death reminds us of the programmed death known in real biological developmental processes.

Our growth and division model may also have relevance to economics, where many individuals or companies compete for finite resources. Growth, division, death (bankrupt) factors are important in economics. Time sharing for resources is useful there. Economic crash may be related with the above multiple cell deaths, and may be due to synchronized behaviors of agents for resources.

The present model, of course, is too simple to the study of cell growth and differentiation. Here we have discussed this model as the simplest illustration. For a model including metabolic reaction, and other stimulating results, see [19] in the present proceeding. In the present model we have not found a state corresponding to the stage III in [19]. Possibly we need at least a model with two variables, phase and amplitude, to have the stage III where separation of poor and rich cells emerges.

8. Summary and discussions

In the present paper we have discussed relevance of dynamic clustering to biological problems. In a network of chaotic elements, they often split into synchronized clusters due to chaotic instability. Identical elements spontaneously differentiate. Thus the clustering can give a basic concept for the origin of diversity. Indeed we have applied the clustering mechanism to cell differentiation in Section 7.

By using a hypercubic topology and local nonlinear dynamics, we have studied clusterings with bit structures. Clusters are spontaneously formed reflecting the bit structure. Relevant bits are spontaneously formed, which opens up the possibility of self-organizing genetic algorithms. Since viruses form quasispecies coded in a hypercubic space as Eigen et al. discusses [35], it may be interesting to search for dynamic clustering there.

When chaotic instability and averaging by couplings are somewhat balanced, a partition into clusters is very complex. In this partially ordered state, dynamics is also complex with chaotic itinerancy over ordered states. Relevance of the partially ordered states and chaotic itinerancy to biological networks have been discussed throughout the paper.

In the hypercubic topology, chaotic switches of relevant bits are formed successively. Besides possible relevance to dynamics of immune net-

works and virus populations, such chaotic itinerancy of bits may be of use in genetic algorithms.

Relevance of the partially ordered states to ecological and immune networks is studied with the inclusion of the change of effective couplings as mutation of mutation rates. It turns out that the system maintains its stability as homeochaos, by forming a feedback mechanism to keep the system around partially ordered states. The homeochaos provides a mechanism of the maintenance of diversity, important in ecological and other biological networks.

In a model allowing for the growth of the number of elements, we have found that effective time sharing system of resources is formed in partially clustered states. A balance between synchronization and desynchronization is necessary here, for the effective use of resources, which enable the growth of the number of cells (agents). This study of growing cells, originally motivated in the cell differentiation and division, may be applied to economics, where a breakdown of the time sharing system by synchronization may lead to economic crash.

In a GCM with synaptic couplings, we have observed the clustering formation through some interference of external inputs and local dynamics. To have a capacity to construct a map of complex environment, it is desirable to have a potentiality of complex partitions to clusters, supported by partially ordered states.

To sum up we have studied classes of extensions of coupled maps to hypercubic topology, synaptic couplings, growing degrees, and so on, in order to understand the origin and maintenance of diversity and complexity in biological networks.

Acknowledgements

I am grateful to Ichiro Tsuda, Takashi Ikegami, Kenji Araki, Hatsuo Hayashi, Ad Aertsen, Hiroyuki Ito, Hiroshi Fujii, Walter Freeman, and Tetsuya Yomo for stimulating discussions. I am again grateful to Takashi Ikegami (for Sections 3 and 4), Kenji Araki (for Section 6), and Tetsuya Yomo (for Section 7), for exciting discussions through collaboration on related (but distinct) works [25,26,33,19]. The work is partially supported by Grant-in-Aids for Scientific Research from the Ministry of Education, Science, and Culture of Japan.

References

[1] I. Tsuda, Chaos-teki-Nou-kan [Chaotic Scenario of Brain] (Saiensu-sha, 1991) [in Japanese].

[2] I.Tsuda, Prog. Theor. Phys. Suppl. 79 (1984) 241

[3] I. Tsuda, Chaotic neural networks and thesaurus, in: Neurocomputers and Attention, A.V. Holden and V.I. Kryukov, eds. (Manchester Univ. Press, Manchester, 1990).

[4] I. Tsuda, Physica D 75 (1994) 165, these proceedings.

[5] W. Freeman and C.A. Skarda, Spatial EEG Patterns, Nonlinear Dynamics and Perception: the Neo-Sherringtonian View, Brain Res. Rev. 10 (1985) 147; W. Freeman, Petit Mal Seizure Spikes in Olfactory Bulb and Cortex Caused by Runaway Inhibition after Exhaustion of Excitation, Brain Res. Rev. 11 (1986) 259.

[6] R. Eckhorn et al., Coherent Oscillations: A mechanism of feature linking in the visual cortex?, Biol. Cybernetics 60 (1988) 121.

[7] C.M. Gray, P. Koenig, A.K. Engel and W. Singer, Oscillatory Responses in cat visual cortex exhibit inter-columnar synchronization which reflects global stimulus properties, Nature 338 (1989) 334.

[8] J. Kruger, ed., Neuronal Cooperativity (Springer, New York, 1991).

[9] A. Aertsen and E. Vaadia, Coding and computation in the cortex: single-neuron activity and cooperative phenomena, in: Information Processing in the Cortex: Experiments and Theory, A. Aertsen A.V. Braitenberg, eds. (Springer, Berlin, Heidelberg, New York, Tokyo, 1992) pp. 81-121;
Ad Aertsen, Physica D 75 (1994) 103, in these proceedings.

[10] C.S. Elton, The Pattern of Animal Communities (Methuen, London, 1966).

[11] R. May, Stability and Complexity in Model Ecosystems (Princeton Univ. Press, Princeton, 1973).

[12] J. Kikkawa, Kagaku 60 (1990) 603 [in Japanese]; J.H. Connel, Science 199 (1978) 1302.

[13] N.K. Jerne, in: The neurosciences: A study program, G.C. Quarton, T. Melnechuk and F.O. Schmitt, eds. (Rockefeller Univ. Press, New York).

[14] J.D. Farmer, N.H. Packard and A.S. Perelson, Physica D 22 (1986) 187.
[15] M. Mezard, G. Parisi and M.A. Virasoro, eds., Spin Glass Theory and Beyond (World Scientific, Singapore, 1988).
[16] T. Ikegami, Prog. Theor. Phys. 81 (1989) 309.
[17] S Kauffman, The Origin of Order (Oxford Univ. Press, Oxford, 1993).
[18] E. Ko, T.Yomo, I. Urabe, Physica D 74 (1994) ???, in these proceedings.
[19] K. Kaneko and T. Yomo, Cell Division, Differentiation, and Dynamic Clustering, Physica D 75 (1994) 89, these proceedings.
[20] K. Kaneko, Phys. Rev. Lett. 63 (1989) 219; Physica D 41 (1990) 137.
[21] K. Kaneko, Phys. Rev. Lett. 65 (1990) 1391; Physica D 55 (1992) 368.
[22] K. Kaneko, J. Phys. A 24 (1991) 2107–2119.
[23] K. Kaneko, Physica D 54 (1991) 5.
[24] K.Ikeda, K. Matsumoto and K. Ohtsuka, Prog. Theor. Phys. Suppl. 99 (1989) 295.
[25] K. Kaneko and T. Ikegami, Homeochaos: Dynamics Stability of a symbiotic network with population dynamics and evolving mutation rates, Physica D 56 (1992) 406–429.
[26] T. Ikegami and K. Kaneko, Evolution of Host-Parasitoid Network through Homeochaotic Dynamics, Chaos 2 (1992) 397–408.
[27] K. Kaneko, Prog. Theor. Phys. 72 (1984) 480; Physica D 34 (1989) 1; Simulating Physics with Coupled Map Lattices – Pattern Dynamics, Information Flow, and Thermodynamics of Spatiotemporal Chaos, in: Formation, Dynamics, and Statistics of Patterns, K. Kawasaki, A. Onuki and M. Suzuki, eds. (World Scientific, Singapore, 1990);
K. Kaneko, ed., Theory and Applications of Coupled Map Lattices (Wiley, New York, 1993).
[28] N. Nakagawa and Y. Kuramoto, Prog. Theor. Phys. 89 (1993) 313; Physica D 75 (1994) 74, in these proceedings.
V. Hakim and W.J. Rappel, Phys. Rev. A 46 (1992) 7347.
[29] K. Kaneko, Hypercubic Coupled Maps, Physica D (1992), to be submitted.
[30] H. Chaté and P. Manneville, Chaos 2 (1992) 307.
[31] J. Holland, Escaping Brittleness, in: Machine Learning II, R.S. Mishalski, J.G. Carbonell and T.M. Miechell, eds. (Kaufman, Los Altos, CA, 1986).
[32] K. Kaneko, Artificial Life 1 (1994), to appear.
[33] See for a related study, K. Araki and K. Kaneko, to be published.
[34] Hatsuo Hayashi, private communication.
[35] M. Eigen, J. McCaskill and P. Schuster, J. Phys. Chem. 92 (1988) 6881.